This article was downloaded by:
On: *14 January 2011*
Access details: *Access Details: Free Access*
Publisher *Taylor & Francis*
Informa Ltd Registered in England and Wales Registered Number: 1072954 Registered office: Mortimer House, 37-41 Mortimer Street, London W1T 3JH, UK

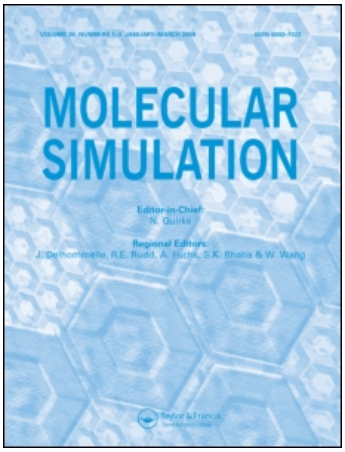

Molecular Simulation
Publication details, including instructions for authors and subscription information:
http://www.informaworld.com/smpp/title~content=t713644482

Self-Diffusion in Electrostatically Stabilized Colloidal Suspensions Using Brownian Dynamics

W. E. Tegrotenhuis[a]; C. J. Radke[a]; M. M. Denn[a]
[a] Center for Advanced Materials, Lawrence Berkeley Laboratory and Department of Chemical Engineering, University of California, Berkeley, California, USA

To cite this Article Tegrotenhuis, W. E. , Radke, C. J. and Denn, M. M.(1989) 'Self-Diffusion in Electrostatically Stabilized Colloidal Suspensions Using Brownian Dynamics', Molecular Simulation, 2: 1, 3 — 14
To link to this Article: DOI: 10.1080/08927028908032780
URL: http://dx.doi.org/10.1080/08927028908032780

PLEASE SCROLL DOWN FOR ARTICLE

Full terms and conditions of use: http://www.informaworld.com/terms-and-conditions-of-access.pdf

This article may be used for research, teaching and private study purposes. Any substantial or systematic reproduction, re-distribution, re-selling, loan or sub-licensing, systematic supply or distribution in any form to anyone is expressly forbidden.

The publisher does not give any warranty express or implied or make any representation that the contents will be complete or accurate or up to date. The accuracy of any instructions, formulae and drug doses should be independently verified with primary sources. The publisher shall not be liable for any loss, actions, claims, proceedings, demand or costs or damages whatsoever or howsoever caused arising directly or indirectly in connection with or arising out of the use of this material.

Molecular Simulation, 1989, Vol. 2, pp. 3–14
Reprints available directly from the publisher
Photocopying permitted by license only

© 1989 Gordon and Breach Science Publishers S.A.
Printed in Great Britain

SELF-DIFFUSION IN ELECTROSTATICALLY STABILIZED COLLOIDAL SUSPENSIONS USING BROWNIAN DYNAMICS

W.E. TEGROTENHUIS, C.J. RADKE, and M.M. DENN

Center for Advanced Materials, Lawrence Berkeley Laboratory and Department of Chemical Engineering, University of California, Berkeley, California 94720 USA

(*Received December 1987; in final form March 1988*)

Brownian dynamics is applied to suspended colloidal particles interacting through a screened Coulombic pair potential in the dilute region where the hydrodynamics is approximated by Stokes drag. Calculated properties include the osmotic pressure, the radial distribution function, and the self-diffusion coefficient. Verification is obtained by comparing the results to independently evaluated properties. Self-diffusion coefficicents are compared to approximate theories in the literature. The self-diffusion coefficient is observed to depend strongly on the local structure but only slightly on the longer range structure.

KEY WORDS: Brownian dynamics, colloidal suspensions, Coulombic potential, self-diffusion coefficient, osmotic pressure.

Downloaded At: 20:00 14 January 2011

1 INTRODUCTION

Detailed knowledge of the microstructure of suspensions is necessary for a comprehensive understanding of macroscopic behavior. The influence of microstructure is manifested in a wide range of rheological behavior, for example shear thinning, thixotropy, dilatancy, and viscosity discontinuity [1–3]. One application in which microstructure plays a critical role is in the production of specialty ceramics, where colloidal suspensions act as precursors; here the microstructure influences structural, thermal, optical, and electrical properties of the ceramic products. In this work, the objective is to study the influence of microstructure on the self-diffusion of colloidal particles.

Brownian dynamics (BD) is a useful tool for studying microstructure. From first principles, Brownian dynamics enables the simulation of the trajectories of a collection of particles at constant temperature and concentration. From the particle trajectories, the dynamics of the microstructure can be discerned and the macroscopic properties calculated [4–9]. Brownian dynamics differs from molecular dynamics in the treatment of the solvent molecules [10,11]. The solvent molecules and the particles differ in size by several orders of magnitude in colloidal suspensions; hence the time scales of motion also differ by several orders of magnitude. The motion of the solvent in Brownian dynamics simulations is integrated over the time scale of the particle motion, and the solvent-solvent and solvent-particle interactions are replaced by a

viscous dissipation term and a random Brownian force, respectively, in the equations of motion for the colloidal particles. These terms are related through the fluctuation dissipation theorem [12,13] and serve to exchange energy between particles and the solvent. In this way the solvent behaves as a thermal bath maintaining the average temperature of the particles.

The particles also experience a potential field due to the presence of the other particles. The sources of these interactions include short range Born repulsion, short range structural forces, van der Waals forces, electrostatic forces, and steric forces; their relative importance depends on the composition and properties of the solvent and the bulk and surface properties of the particles. When the surfaces of the particles are charged and in an aqueous solvent at low ionic strength, the electrostatic repulsive force is the dominant interaction; for this class of systems, the screened Coulombic pair potential [14] is typically used [5–9,15,16]. Because they are moving through a viscous medium, the particles can also interact hydrodynamically; at sufficiently low concentrations, with large, long-range repulsive forces, the hydrodynamic interactions are negligible, however.

In this work, the overall system is stationary and at constant uniform conditions. Thermodynamic properties can therefore be calculated, enabling verification of the technique by comparison with other evaluations of thermodynamic properties. The calculated self-diffusion coefficients, obtained as the limiting slope of the mean square displacement curve, enable the evaluation of the applicability of available theories for self-diffusion. The influence of microstructure on self-diffusion is discerned by varying simulation parameters and contrasting the changes in the self-diffusion coefficient with changes in the radial distribution function.

Downloaded At: 20:00 14 January 2011

2 THEORY

The Brownian dynamics method employs the Langevin equation as the equation of motion for the particles [11]. The force balance includes inertia, viscous drag, interparticle forces, and a random Brownian force, respectively, as follows:

$$m\mathbf{a}_i + \mathbf{R}\cdot\mathbf{v}_i - \mathbf{F}_i - m\mathbf{A}_i = 0 \tag{1}$$

Here m is the particle mass; $\mathbf{a}_i$ and $\mathbf{v}_i$ are the acceleration and velocity vectors of particle i, respectively; $\mathbf{R}$ is the resistance matrix; $\mathbf{F}_i$ is the net interparticle force; and $\mathbf{A}_i$ is the random Brownian force.

Each particle moves through a potential field resulting from the presence of other particles in the system. Particle i therefore experiences a net force, $\mathbf{F}_i$, which depends on the instantaneous location of the other particles; we assume pairwise additivity,

$$\mathbf{F}_i = \sum_j -\frac{dU(r_{ij})}{dr}\frac{\mathbf{r}_{ij}}{r_{ij}} \tag{2}$$

where the sum is over all the other particles and $U(r)$ is the potential of interaction between two particles with centers separated by distance r. The potential,

$$U(r) = U_o\frac{\exp(-(r-2a)/\lambda)}{r} \tag{3}$$

is used throughout this work to model the interaction between electrostatically stabilized particles; this form is equivalent to the screened Coulombic interaction of

the DLVO theory [14] in the limit of $\lambda/a \gg 1$, where λ is the Debye screening length and a is the particle radius. Other interactions are assumed to be negligible in this limit. U_o is, in general, a function of the particle surface potential (or surface charge), the permittivity of the solvent, and the particle radius. The Debye screening length is a defined function of the ionic concentration, the solvent permittivity, and the temperature.

The resistance matrix, $\mathbf{R}$, contains the hydrodynamic interactions between the particles and is in general a function of the instantaneous particle configuration [17,18]. At low concentration, in the limit of $\lambda/a \gg 1$ and $U_o/kT \gg 1$, the particles do not approach closely enough to experience significant hydrodynamic interactions. Viscous drag is therefore approximated by Stokes drag; accordingly, the resistance matrix is set to

$$\mathbf{R} = \frac{kT}{D_o}\mathbf{I} \tag{4}$$

where $\mathbf{I}$ is the identity matrix. D_o is the free diffusion coefficient which is obtained from the Stokes-Einstein relationship

$$D_o = \frac{kT}{6\pi\mu a} \tag{5}$$

where μ is the solvent viscosity. The systems are at sufficiently low concentration to justify the Stokes drag assumption for most of the results, but for the purpose of comparison to theory, results have been included for higher concentrations where the assumption is expected to break down.

Ermak and McCammon developed a numerical solution of the Langevin equation for time steps much greater than the momentum relaxation time [11]. When the Stokes assumption is applied to their result, the particle displacement equation becomes

$$\Delta\mathbf{r}_i = \frac{D_o}{kT}\mathbf{F}_i\Delta t + \mathbf{B}_i. \tag{6}$$

This result states that inertia does not contribute to order Δt with the Stokes drag assumption. It is also obtained from the Smoluchowski equation under the same assumptions [19]. A lemma proved by Chandrasekhar [20] has been used to integrate the random Brownian force, $\mathbf{A}_i$, to give a Gaussian random displacement, $\mathbf{B}_i$, with mean zero and a variance

$$\langle \mathbf{B}_i(\Delta t)\cdot\mathbf{B}_i(\Delta t)\rangle = 2D_o\Delta t. \tag{7}$$

Simulations are performed in three dimensions for a fixed number of particles in a cubic box of length L, using periodic boundary conditions. The long-range forces are truncated using either the spherical cut-off or the minimum image method [21]. Truncation occurs at the surface of a sphere of radius L_s in the former method, and the spherical symmetry is useful in calculating the osmotic pressure correction as given below. The minimum image method, used for comparison, normally truncates the forces at the surface of a cubic box of the same size as the system box and centered at the particle. Here the truncation box is made arbitrarily smaller by specifying half the box length, L_b. Both L_s and L_b must be less than or equal to half the system dimension.

Thermodynamic properties are calculated from particle configurations obtained during the simulation. The radial distribution function, $g(r)$, follows by discretizing the space around each particle into spherical shells

Downloaded At: 20:00 14 January 2011

$$g((r_i + r_{i+1})/2) = \frac{a^3}{\phi(r_i^3 - r_{i+1}^3)} \frac{1}{N_c N} \sum_{j=1}^{N_c} \sum_{k=1}^{N} n_{jk}(r_i, r_{i+1}). \quad (8)$$

Here ϕ is the volume fraction; r_i and r_{i+1} are the inner and outer radius of shell i, respectively; N_c is the number of configurations; N is the number of particles; and n_{jk} is the number of particles in shell i around particle k of configuration j.

The osmotic pressure is calculated using the virial theorem [22] as

$$\frac{\Pi}{\varrho kT} = 1 + \frac{1}{N_c} \sum_{i=1}^{N_c} \left(\frac{1}{3NkT} \sum_{i<j} \mathbf{F}_{ij} \cdot \mathbf{r}_{ij} \right) + \frac{\Pi_a}{\varrho kT} \quad (9)$$

where the second sum is over all particle pairs. Truncation of the pair forces results in underprediction of the osmotic pressure, and a correction, denoted Π_a, is required to account for the long range mean field. This correction is calculated from the pressure equation by assuming that $g(r)$ is equal to unity for distances greater than the truncation length, resulting in the integral

$$\frac{\Pi_a}{\varrho kT} = \frac{\varrho}{6kT} \int_{L_s}^{\infty} r \left(- \frac{dU(r)}{dr} \right) 4\pi r^2 dr \quad (10)$$

when the forces are truncated spherically.

The long-time self-diffusion coefficient, D_s, is defined as the limiting slope of mean-square displacement versus time [9]

$$D_s = \lim_{t \to \infty} \langle (\Delta r(t))^2 \rangle / 6t. \quad (11)$$

The angular brackets indicate an average mean-square displacement for a time interval, t, which is obtained by averaging over many starting times, t^o, and over all the particles [9]. The starting times are separated by a specified number of time steps, m, and the number of starting times, N_o, is determined by the length of the simulation. The average mean-square displacement at a discrete value of time is therefore calculated as

$$\langle (\Delta r(t))^2 \rangle = \frac{1}{N_o N} \sum_{j=1}^{N_o} \sum_{i=1}^{N} | r_i(t + t_j^o) - r_i(t_j^o) |^2. \quad (12)$$

3 CALCULATIONS

All physical and numerical parameters have been non-dimensionalized as shown in Table 1. Results are presented for two sets of the interaction parameters, F_o (the

Table 1 Dimensionless Simulation Parameters

Force constant	$F_o = U_o/2akT$
Debye length	λ/a
Time step	$\Delta\tau = 2D_o\Delta t/a^2$
Volume fraction	$\phi = \frac{4\pi}{3} \frac{N}{(L/a)^3}$
Box truncation length	L_b/a
Sphere truncation length	L_s/a

Downloaded At: 20:00 14 January 2011

Table 2 *GSVW cases*

Case	L_b/a	L_s/a	D_s/D_o	r_{max}/a	$g(r_{max})$
A	–	91.02	0.455	32	1.64
B	–	85.00	0.449	32	1.62
*C	–	80.00	0.432	31.5	1.58
D	–	70.00	0.456	32	1.63
*E	–	60.00	0.419	31.5	1.63
F	–	50.00	0.459	31.5	1.59
G	–	25.00	0.599	26	1.67
H	–	10.00	0.976	–	–
I	91.02	–	0.465	32	1.66
*J	80.00	–	0.427	32	1.59
*K	60.00	–	0.236	31.5	1.61
L	54.50	–	0.2276	36	1.19

Common GSVW parameters:

Force constant	$F_o = 556.$	
Debye length	$\lambda/a = 13.41$	
Box length	$L/a = 182.0$	$(L/a(case\ L) = 108.9)$
Volume fraction	$\phi = 0.00015$	$(\phi(case\ L) = 0.0007)$
Number of particles	$N = 216$	
Time step	$\Delta\tau = 0.3612$	$(\Delta\tau(case\ L) = 0.1806)$
Number of time steps	*4500 or *5000 steps*	
Configuration sampling freq.	*10 steps*	
Starting time, t°, freq.	$m = 10$ *steps*	

dimensionless force constant) and λ/a (the dimensionless Debye screening length). Values $F_o = 556.1$ and $\lambda/a = 13.41$ enable comparison of this work to the Brownian dynamics calculations of Gaylor *et al.* (GSVW) [6,7]. The second parameter set, $F_o = 20.50$ and $\lambda/a = 11.111$, enables comparison of calculated self-diffusion coef-

Table 3 KH cases

Case	ϕ	L/a	D_s/D_o	r_{max}/a	$g(r_{max})$	$\Pi_a/\rho kT$	$\Pi/\rho kT$	$*1 + B_2\varrho$
M	1.6×10^{-5}	406.4	0.968	–	–	2×10^{-7}	1.094	1.10
N	3.2×10^{-5}	322.6	1.012	–	–	1.2×10^{-5}	1.200	1.2
O	8×10^{-5}	237.7	0.907	–	–	8.2×10^{-4}	1.480	1.50
P	0.0005	129.0	0.856	22	1.01	0.247	4.839	4.13
Q	0.001	102.4	0.782	16.5	1.02	1.152	9.083	7.26
R	0.0015	89.42	0.768	15	1.04	2.542	13.41	10.39
S	0.0025	75.42	0.736	12.5	1.07	6.284	22.17	15.65
T	0.005	59.86	0.663	9.5	1.09	18.79	44.38	31.30
U	0.01	47.51	0.667	7.7	1.14	49.96	89.18	62.59
V	0.05	27.78	0.596	4.4	1.27	360.1	449.9	313.0

Common KH parameters:

Force constant	$F_o = 20.50$
Debye length	$\lambda/a = 11.11$
Spherical trunc. length	$L_s/a = (L/a)/2$
Number of particles	$N = 256$
Time step	$\Delta\tau = 0.05$
Number of time steps	*5000 steps*
Configuration sampling freq.	*10 steps*
Starting time, t° freq.	$m = 10$ *steps*

*B_2-Second virial coefficient [22]

Downloaded At: 20:00 14 January 2011

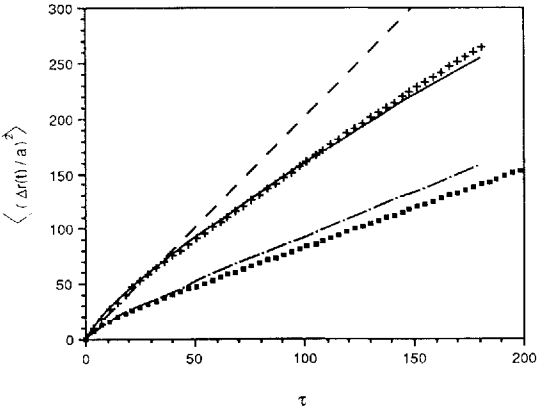

Figure 1 Mean square displacement versus dimensionless time for GSVW parameters (F_o = 556, λ/a = 13.41) at ϕ = 0.015% (——— GSVW [7], + case A), at ϕ = 0.07% (—·— GSVW [7], ■ case L), and for free diffusion (– – –).

Downloaded At: 20:00 14 January 2011

ficients to the theoretical results of Klein and Hess (KH) [15,16]. The volume fraction of particles is varied for a fixed number of particles by varying the box size. The GSVW results were obtained for 216 particles and the KH results for 256 particles. Tables 2 and 3 contain additional simulation information regarding the choice of time step, run length, and the other numerical parameters.

The initial configuration of the particles is obtained as the final configuration of a previous simulation run at the same conditions. The length of the previous simulation was always sufficient to allow the osmotic pressure to reach an asymptotic value. In general, the fluctuations in the osmotic pressure indicate an error of less than 1% in the calculated osmotic pressure (not including the error associated with the correction, Π_a).

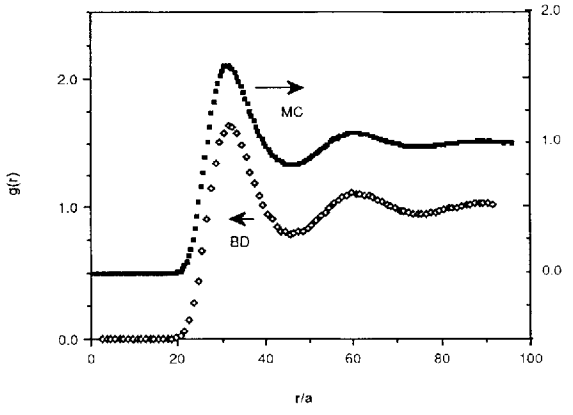

Figure 2 Radial distribution functions calculated for GSVW parameters (F_o = 556, λ/a = 13.41) at ϕ = 0.015% from Brownian dynamics (BD, ◇ – case A) and from Monte Carlo (MC, ■) calculations of E. Reiner [25].

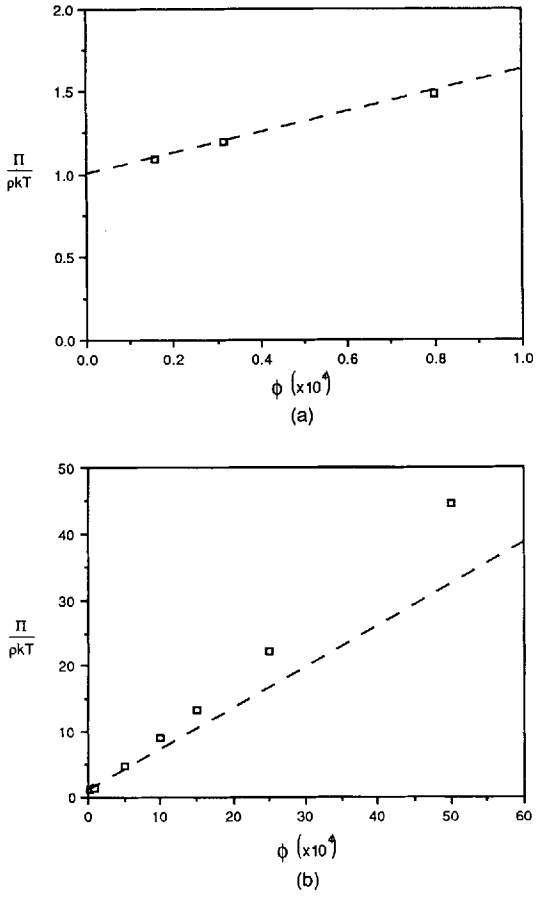

Figure 3 Osmotic pressure versus volume fraction for KH parameters (F_v = 20.5, λ/a = 11.111) from Brownian dynamics calculations (⊡ – including correction, $\Pi_a/\varrho kT$) compared to the linear form of the virial expansion (– – – B_2 = 26200).

Random Brownian displacements are generated using a pseudo-random number generator. First, random numbers are generated from an even distribution on the interval [0,1] using MATLIB's RANF function [23]. They are then converted to a normal distribution with a mean of zero and a standard deviation of unity using the Box-Muller transformation [24]. Finally, the numbers are multiplied by the desired standard deviation, $\sqrt{\Delta\tau}$. A different seed is used to initialize the random number generator for each simulation. Comparisons of simulations run at indentical conditions with different random number sequences indicate errors of up to 5% in the self-diffusion coefficient.

Table 2 contains information for the GSVW simulations including the requisite parameters, the height and location of the first peak in the calculated $g(r)$, and the self-diffusion coefficient. The same information as well as the osmotic pressure is presented in Table 3 for the KH simulations.

Figures 1 to 3 establish the validity of the algorithm. Figure 1 illustrates the

Downloaded At: 20:00 14 January 2011

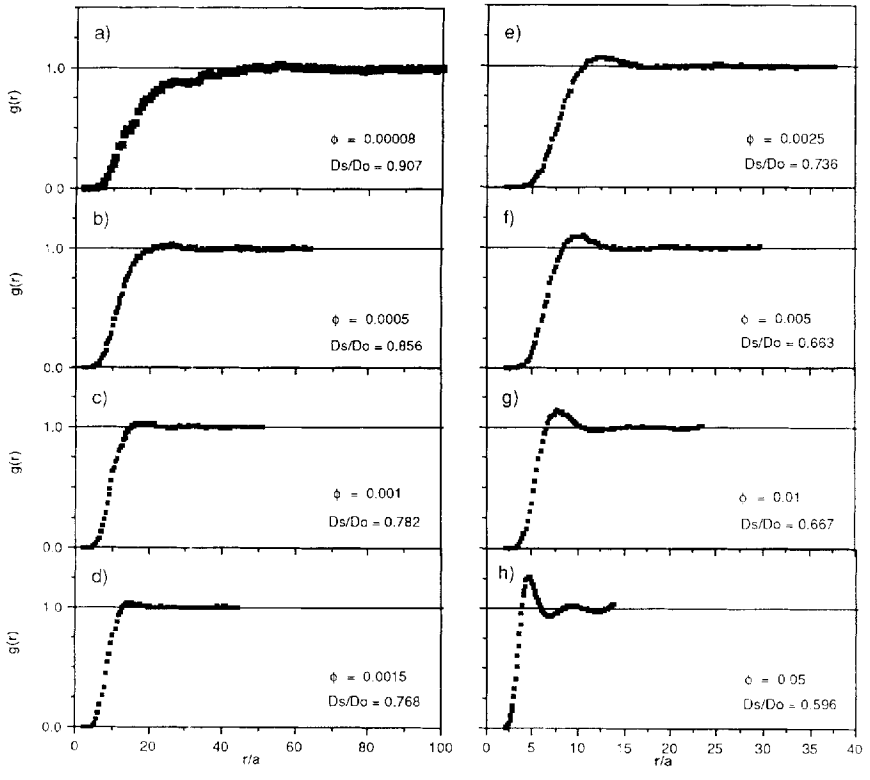

Figure 4 Radial distribution functions calculated for the KH parameters ($F_0 = 20.5$, $\lambda/a = 11.111$) at indicated volume fractions. Forces are spherically truncated at the last calculated $g(r)$ point (Note the change of abscissa scale).

agreement between our calculated mean square displacements and the Brownian dynamics results of Gaylor *et al.* [7] at two volume fractions. A radial distribution function computed using Brownian dynamics is compared in Figure 2 to a result obtained from Monte Carlo calculations [25]; the curves agree within 1% at all points. Finally, the calculated osmotic pressure must agree with the virial expansion in the limit of vanishingly small volume fraction. As shown in Figure 3, there is excellent agreement with the linear virial expansion for the KH parameters up to a volume fraction of about 5×10^{-4} and a value of 5 in the reduced osmotic pressure. (The calculated osmotic pressure deviates positively from the linear form of the virial expansion. This is expected for a purely repulsive system, because the higher order terms in the virial expansion will also have positive coefficients. It is interesting to note from Table 3 that at sufficiently high concentrations the mean field correction becomes the major contribution to the osmotic pressure.)

4 SELF-DIFFUSION COEFFICIENT

Figures 4 and 5 show how the radial distribution function and the self-diffusion coefficient change as the volume fraction is increased beyond the dilute limit. Taken

Downloaded At: 20:00 14 January 2011

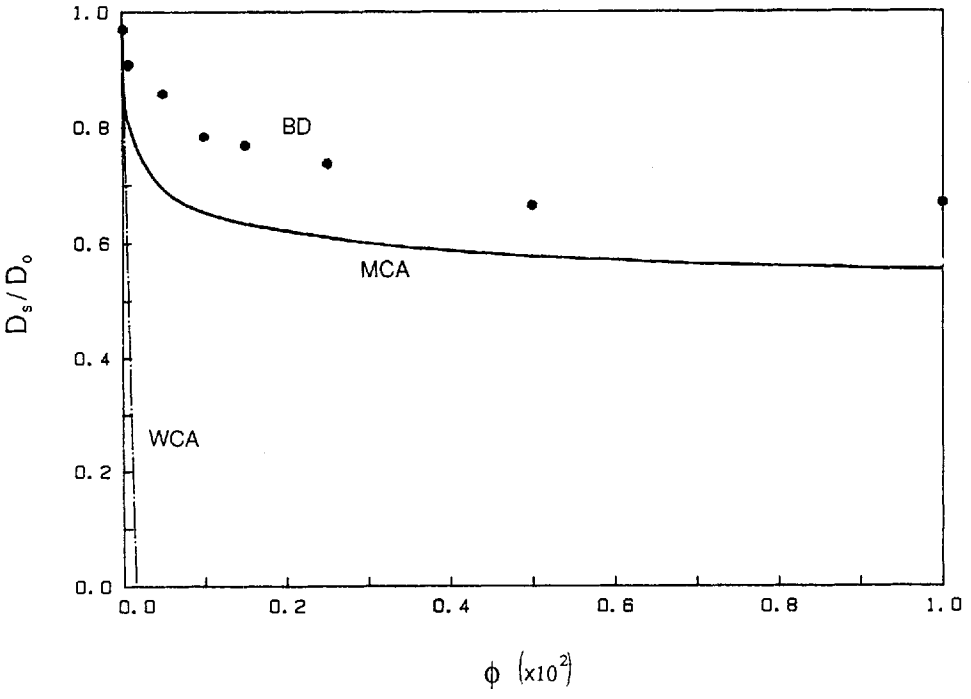

Figure 5 Self-diffusion coefficient, D_s, versus volume fraction for the KH parameters (F_o = 20.5, λ/a = 11.111); weak coupling approximation (—·— WCA) [26], mode coupling approximation (—— MCA) [15, 16], and Brownian dynamics (● BD) results.

together, the two figures illustrate the connection between the appearance of structure in the system and a change in self-diffusion behavior. At very low volume fraction (Fig. 4a), the lack of structure in the system is confirmed by the absence of peaks in $g(r)$; the corresponding self-diffusion coefficient is nearly equal to the free-diffusion coefficient. The gradual development of the first peak in $g(r)$ with increasing volume fraction corresponds to a gradual decrease in the self-diffusion coefficient (Figs. 4b to 4d). Once the first peak has been established, it grows and moves closer to the central particle with increasing volume fraction; D_s continues to decrease, but the rate of decrease is small (Figs. 4e to 4g). Even as the volume fraction is increased to 0.05 (Fig. 4h), where second and possibly third peaks in $g(r)$ appear, the decrease in the self-diffusion coefficient is slight. The self-diffusion coefficient is thus strongly influenced by the presence of a cage of nearest neighbors, but is affected much less by the longer range structure.

Although the calculations are sufficiently accurate to resolve the linear region of the osmotic pressure, which extends to a volume fraction of 5×10^{-4} for the KH parameters (c.f. Fig. 3), the same is not true for the self-diffusion coefficient. Figure 5 shows that the linear weak coupling approximation (WCA) theory [26] for self-diffusion breaks down at an order of magnitude lower in volume fraction; the accuracy of computing D_s is not sufficient at these lower concentrations to establish quantitative comparison. Whereas the virial expansion gives the exact linear behavior,

Downloaded At: 20:00 14 January 2011

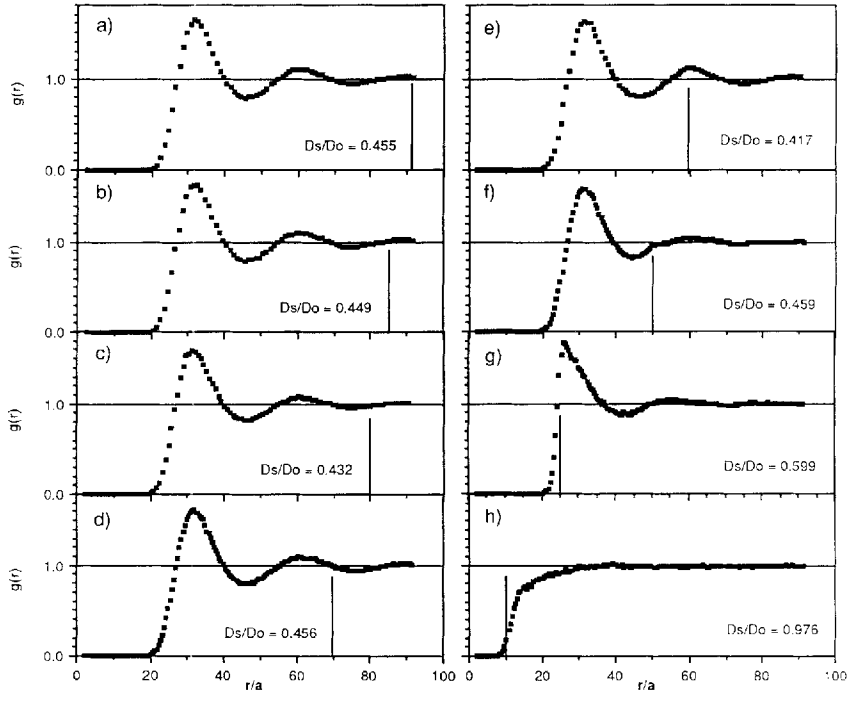

Figure 6 Radial distribution functions calculated for GSVW parameters (F_o = 556, λ/a = 13.41) at ϕ = 0.015% for various spherical force truncation lengths, L_c, indicated by the vertical line in each graph.

the WCA theory relies on the approximation that the potential of interaction is small, and this is only true at very low volume fraction when the particles are typically far apart. As the first peak in $g(r)$ appears at $\phi \sim 5 \times 10^{-4}$, the particle interactions become strong, so the weak coupling theory must break down.

Klein and Hess predicted non-linear dependence of the self-diffusion coefficient on volume fraction by using a mode coupling approximation to incorporate equilibrium structure [15, 16]. Figure 5 demonstrates the ability of the mode coupling theory to predict the correct qualitative behavior; the large decrease in D_s in the region where the first peak of $g(r)$ appears is followed by a gradual decrease at higher volume fractions. The mode coupling theory results are 10–20% lower than the Brownian dynamics results.

Ohtsuki and Okano [27, 28] predicted self-diffusion coefficients by using the superposition approximation and solving the Smoluchowski diffusion equation to first order in particle density. Their results are in quantitative agreement with Brownian dynamics calculations of Gaylor *et al.* [6, 7]. Ohtsuki [27] observed that the self-diffusion coefficient continues to slowly decrease for very long times and suggested that the Brownian dynamics calculations have not achieved the limiting slope of the mean-square displacement, resulting in an overprediction of the long-time self-diffusion coefficient. Klein and Hess [29] have reported similar behavior. This is a possible explanation for the quantitative disagreement in the results.

The influence of the truncation of the forces on $g(r)$ and D_s is illustrated in Figs.

Downloaded At: 20:00 14 January 2011

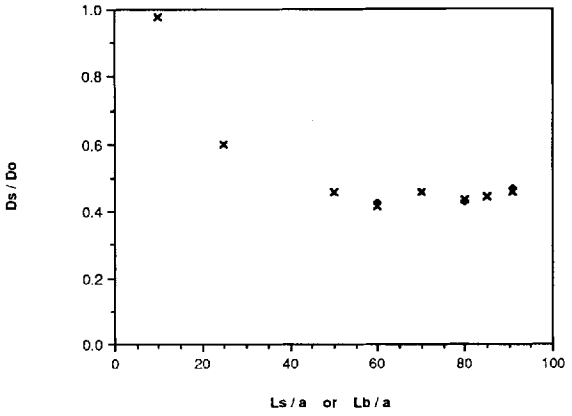

Figure 7 Self-diffusion coefficient versus force truncation length (x - L_s, spherical; ◆ - L_b, box) for GSVW parameters (F_0 = 556, λ/a = 13.41) at ϕ = 0.015%.

6 and 7. When L_s is beyond the second peak in $g(r)$, changing the force truncation length has a minimal effect on both $g(r)$ and D_s (Figs 6a to 6e). When the truncation length is moved inside the second peak, the structure of the second peak is effectively lost, but the self-diffusion coefficient remains relatively uneffected (Fig. 6f). A significant change in self-diffusion is not observed until the truncation length is reduced to the location of the first peak in $g(r)$ (Fig. 6g). Finally, when the truncation length is less than the location of the first peak, the structure of the system is completely lost and the free diffusion coefficient is recovered. The comparison of the spherical cut-off and minimum image methods shown in Figure 7 demonstrates that the choice of the truncation shape does not influence the computed self-diffusion coefficient as long as the truncation length is sufficiently large. This provides a further illustration of the fact that self-diffusion is strongly dependent on the local structure and is only slightly influenced by long-range structure.

Downloaded At: 20:00 14 January 2011

Acknowledgment

This work was supported by the Director, Office of Energy Research, Office of Basic Energy Sciences, Materials Science Division of the U.S. Department of Energy under Contrast No. DE-AC03-76SF00098. We have benefited from discussions with Eric Reiner and Jan Mewis; the latter were made possible by a NATO grant. Computations were performed on a Cray-XMP machine located at the NMFE computer center, Lawrence Livermore Laboratories and the Cray-XMP machine located at the San Diego Supercomputer Center.

References

[1] J. Mewis and A.J.B. Spaull, "Rheology of Concentrated Dispersions", *Adv. Colloid Interface Sci.*, **6**, 173–200, (1976).

[2] W.B. Russel, "Review of the Role of Colloidal Forces in the Rheology of Suspensions", *J. Rheol.*, **24**(3), 287–317, (1980).

[3] R.L. Hoffman, "Discontinuous and Dilatant Viscosity Behavior in Concentrated Suspensions. I. Observation of a Flow Instability", *Trans. Soc. Rheol.*, **16**(1), 155–173, (1972).

[4] I.K. Snook, W. van Megen, K.J. Gaylor, and R.O. Watts, "Computer Simulation of Colloidal Dispersions", *Adv. Colloid Interface Sci.*, **17,** 33–49, (1982).
[5] K.J. Gaylor, I.K. Snook, W.J. van Megen, and R.O. Watts, "Dynamics of Colloidal Systems: Time-dependent Structure Factors", *J. Phys. A.*, **13,** 2513–2520, (1980).
[6] K.J. Gaylor, I.K. Snook, W. van Megen, and R.O. Watts, "Brownian Dynamics Studies of Dilute Dispersions", *Chem. Phys.*, **43,** 233–239, (1979).
[7] K.J. Gaylor, I.K. Snook, W. van Megen, and R.O. Watts, "Brownian Dynamics of Many-Body Systems", *Faraday Trans. II*, **76,** 1067–1078, (1980).
[8] W. van Megen and I. Snook, "Diffusion in Concentrated Monodisperse Colloidal Solutions. The Hard Sphere – Thermodynamic or Hydrodynamic?", *Faraday Discuss. Chem. Soc.*, **76,** 151–163, (1983).
[9] W. van Megen and I. Snook, "Brownian-dynamics Simulation of Concentrated Charge-Stabilized Dispersions. Self-Diffusion.", *Faraday Trans.* **80,** 383–394, (1984).
[10] J.M. Deutch and I. Oppenheim, "Molecular Theory of Brownian Motion for Several Particles", *J. Chem. Phys.*, **54**(8), 3547–3555, (1971).
[11] D.L. Ermak and J.A. McCammon, "Brownian Dynamics with Hydrodynamic Interactions", *J. Chem. Phys.*, **69**(4), 1352–1360, (1978).
[12] G. Bosis, B. Quentrec, and J.P. Boon, "Brownian Dynamics and the Fluctuation-Dissipation Theorem", *Molec. Phys.*, **45**(1), 191–196, (1982).
[13] T. Akesson and B. Jonsson, "Brownian Dynamics Simulation of Interacting Particles", *Molec. Phys.*, **54**(2), 369–381, (1985).
[14] E.J.W. Verway and J.T.G. Overbeek, *Theory of the Stability of Lyophobic Colloids*, Elsevier, Amsterdam, 1948.
[15] W. Hess and R. Klein, "Generalized Hydrodynamics of Systems of Brownian Particles", *Adv. Phys.*, **32**(2), 173–283, (1983).
[16] R. Klein and W. Hess, "Mass-diffusion and Self-diffusion Properties in Systems of Strongly Charged Spherical Particles", *Faraday Discuss. Chem. Soc.*, **76,** 137–150, (1983).
[17] J. Happel and H. Brenner, *Low Reynolds Number Hydrodynamics*, Martinus Nijhoff Publishers, Dordrecht, The Netherlands, 1983.
[18] H. Brenner and M.E. O'Neill, "On the Stokes Resistance of Multiparticle Systems in a Linear Shear Field", *Chem. Eng. Sci.*, **27,** 1421–1439, (1972).
[19] D.L. Ermak, "A Computer Simulation of Charged Particles in Solution. I. Technique and Equilibrium Properties", *J. Chem. Phys.*, **62,** (10), 4189–4196, (1975).
[20] S. Chandrasekhar, "Stochastic Problems in Physics and Astronomy. Ch. 2. The Theory of the Brownian Motion", *Rev. Mod. Phys.*, **15,** 20–44, (1943).
[21] D. Levesque, G.N. Patey, and J.J. Weiss, " A Monte Carlo Study of Dipolar Hard Spheres. The Pair Distribution Function and the Dielectric Constant", *Molec. Phys.*, **34**(4), 1077–1091, (1977).
[22] J.O. Hirschfelder, C.F. Curtiss, and R.B. Bird, *Molecular Theory of Gases and Liquids*, Wiley, NY 1966, pp. 41–43, 134–136.
[23] A description of the MATHLIB subroutine package is available from the National Magnetic Fusion Energy Computer Center, Lawrence Livermore Labs, Livermore, CA.
[24] G. Dahlquist and A. Bjorck, *Numerical Methods*, Prentice-Hall, Inc., New Jersey, 1974, pp. 453–454.
[25] E.S. Reiner, Ph.D. Dissertation, University of California at Berkeley (in progress).
[26] J.A. Marqusee and J.M. Deutch, "Concentration Dependence of the Self-diffusion Coefficient", *J. Chem. Phys.*, **73**(10), 5396–5397, (1980).
[27] T. Ohtsuki, "Dynamical Properties of Strongly Interacting Brownian Particles", *Physica*, **110A,** 606–616, (1982).
[28] T. Ohtsuki and K. Okano, "Diffusion Coefficients of Interacting Brownian Particles", *J. Chem. Phys.*, **77**(3), 1443–1450, (1982).
[29] W. Hess and R. Klein, "Dynamical Properties of Colloidal Systems III. Collective and Self-Diffusion of Interacting Charged Particles", *Physica*, **105A,** 552–576, (1981).

Downloaded At: 20:00 14 January 2011